JOURNAL OF CATALYSIS 146, 268–277 (1994)

Molecular Structures and Reactivity of Supported Molybdenum Oxide Catalysts

Du Soung Kim,*[,1] Israel E. Wachs,*[,2] and Kohichi Segawa†

*Zettlemoyer Center for Surface Studies, Department of Chemical Engineering, Lehigh University, Bethlehem, Pennsylvania 18015; and †Department of Chemistry, Faculty of Science and Technology, Sophia University, 7-1 Kioi-cho, Chiyoda-ku, Tokyo 102 Japan

Received August 20, 1993; revised March 16, 1994

Supported molybdenum oxide catalysts were prepared by an equilibrium adsorption method. The molecular structures of the molybdenum oxide overlayers on different oxide supports (Al_2O_3, TiO_2, ZrO_2, SiO_2, and MgO), under *in situ* conditions, were investigated by Raman spectroscopy. The molybdenum oxide species on TiO_2, ZrO_2, and Al_2O_3 possess a highly distorted, octahedrally coordinated surface molybdenum oxide species with one short Mo=O bond regardless of the molybdenum oxide content. The MoO_3/SiO_2 catalysts primarily contain crystalline MoO_3 because of the lower density and reactivity of the silica surface OH groups. The MoO_3/MgO catalysts possess $MgMoO_4$ and $CaMoO_4$ compounds due to the high aqueous solubility of MgO and CaO (an impurity in the MgO support) and the strong acid–base interaction between molybdenum oxide and MgO/CaO. The methanol oxidation reaction studies revealed that the MoO_3/TiO_2 (anatase and rutile) and MoO_3/ZrO_2 catalysts are the most active catalysts and that their activities (TOFs) are at least 1–2 orders of magnitude higher than those of the MoO_3/Al_2O_3, MoO_3SiO_2, and MoO_3/MgO catalysts. It was also found that the catalytic activities correlate with the reducibility of the surface molybdenum oxide species on the oxide supports as well as their surface morphology (e.g., molybdenum oxide dispersion and molybdate compound formation). These studies demonstrate that the specific oxide support controls the reactivity of the supported molybdenum oxide phases.

INTRODUCTION

Supported molybdenum oxide catalysts have been extensively investigated because of their numerous catalytic applications in petroleum, chemical, and pollution control industries (1). These catalysts are usually prepared by depositing the catalytically active molybdenum oxide component on the surface of an oxide support (Al_2O_3, TiO_2, ZrO_2, SiO_2, and MgO). The industrial importance of supported molybdenum oxide catalysts has motivated a large number of studies concerning the surface structures of the molybdenum oxide species by Fourier transform infrared (FTIR) (2a, 3), ultraviolet visible diffuse reflectance (UV-vis) (2a, 2b, 4–5), extended X-ray absorption fine structure (EXAFS) (6–11), X-ray absorption near edge structure (XANES) (8), ^{95}Mo nuclear magnetic resonance (NMR) (12–16), and Raman spectroscopies (2–4, 8, 16–36).

Not all the spectroscopic measurements, however, have resulted in definitive structural determinations of the supported molybdenum oxide species. FTIR can in principle provide structural information about the surface molybdenum oxide species, but strong absorption of the IR signal by the oxide support below 1000 cm^{-1} limits the collection of spectra in this region, while UV-vis cannot provide detailed structural information on the surface molybdenum oxide species due to its broad UV features (17a). EXAFS can discriminate between different metal oxide structures, but this technique averages the signal from all sites and makes it very difficult to differentiate between the several structures that may simultaneously be present in the catalyst. XANES can provide information about the coordination number of the molybdenum oxide species (tetrahedral or octahedral coordination), but it also has difficulty discriminating between different structures possessing the same coordination number because it also averages the signal from all sites. Solid-state ^{95}Mo NMR can provide detailed structural information of the supported molybdenum oxide species, but the low sensitivity of the ^{95}Mo NMR signal generally makes it difficult to obtain meaningful signals. More recent solid state ^{95}Mo NMR studies of supported molybdenum oxide catalysts, however, appear very promising (15). Recently, Raman spectroscopic studies have provided detailed information concerning the surface structures of the molybdenum oxide species on oxide supports. The advantage of Raman spectroscopy is that it can discriminate between the different molecular states of the supported metal oxide

[1] Present address: Research and Development Division, Daelim Engineering Co., Ltd., #17-5 Yoido-dong, Yongdungpo-ku, Seoul, 150-010 Korea.

[2] To whom correspondence should be addressed.

0021-9517/94 $6.00

since each state possesses a unique vibrational spectrum that is directly related to its structure.

A large number of studies concerning the surface structures of the supported molybdenum oxide species have been investigated by Raman spectroscopy (2–4, 8, 16–36). However, only a limited number of these investigations have been reported under *in situ* dehydrated conditions (2a, 8, 17, 19–21, 30, 34–36). It is generally accepted that the symmetric stretching mode of the terminal Mo=O bond at 940–960 cm^{-1} under hydrated conditions shifts to the higher wavenumber region (980–1000 cm^{-1}) upon dehydration at elevated temperatures. However, there is still disagreement regarding the assignment of the Raman band shift to higher wavenumber upon dehydration. Therefore, a systematic study is required in order to understand the surface structures of the supported molybdenum oxide species under *in situ* dehydrated conditions.

The surface morphology of heterogeneous catalysts can influence the catalytic activity and selectivity of partial oxidation reactions. For example, methanol oxidation is well known as a reaction which is sensitive to the surface properties of metal oxides (37–39), and it is used as a model reaction to characterize the surface properties of catalysts (40, 41) as well as the interactions between the deposited surface oxide and the oxide support (33c, 42, 43). The present study investigates the surface structures of molybdenum oxide species on oxide supports (Al_2O_3, TiO_2, ZrO_2, SiO_2, and MgO) under *in situ* dehydrated conditions and the influence of the specific support on the reactivity and selectivity of the molybdenum oxide species during methanol oxidation.

EXPERIMENTAL

Catalyst preparation. The oxide supports used in this study are Al_2O_3 (JRC-AlO-4), TiO_2 (anatase, Idemitsu UFP TiO_2), TiO_2 (rutile, JRC-TiO-3), ZrO_2, SiO_2 (Degussa, Aerosil-200), and MgO (JRC-MgO-1). The Al_2O_3, TiO_2 (rutile), and MgO supports employed were Japan Reference Catalysts (JRC) (44) and ZrO_2 was prepared by the method of Tanabe and co-workers (45). The TiO_2 (anatase) support was obtained by calcining the amorphous Idemitsu UFP TiO_2 at 773 K for 2 h. The supported molybdenum oxide catalysts were prepared by the equilibrium adsorption method with an aqueous solution of ammonium heptamolybdate ($(NH_4)_6Mo_7O_{24} \cdot 4H_2O$). Further details of the preparation are given elsewhere (2, 16, 31, 40). The adsorbed amounts of molybdenum (wt% MoO_3) were determined by inductively coupled plasma emission spectroscopy (ICPES, Seiko Denshi, SPS-1100). For ICPES measurement, 0.2 g of the sample was fused with K_2SO_4 and dissolved with a diluted H_2SO_4 solution.

BET surface area and CO_2 chemisorption. Both experiments were carried out on a standard volumetric BET adsorption system. The BET surface areas of the catalysts were determined by N_2 adsorption at 77 K. The CO_2 adsorption isotherms of the catalysts were measured at 293 K. Adsorption isotherms of Langmuir type have been obtained for all catalysts. The CO_2 chemisorption of each catalyst was determined at the extrapolated pressure of zero.

Raman spectroscopy. The Raman spectra of the supported molybdenum oxide catalysts under *in situ* dehydrated conditions were obtained with an Ar^+ ion laser (Spectra Physics Model 2020-50) delivering about 15–40 mW of incident radiation. The excitation line of the laser was 514.5 nm. The scattered radiation from the sample was directed into a Spex Triplemate spectrometer (Model 1877) coupled to a Princeton Applied Research OMA III optical multichanneled analyzer (Model 1463) equipped with an intensified photodiode array detector cooled thermoelectrically to 243 K. The spectral resolution and reproducibility were experimentally determined to be better than 2 cm^{-1}. For the *in situ* dehydration experiment, a modified version of the *in situ* cell developed by Wang was used (2). Prior to the Raman measurement, the catalysts were dehydrated at 773 K for 1 h in flowing O_2 and cooled to room temperature. Ultra-high-purity, hydrocarbon-free oxygen (Linde gas) was purged through the cell during the acquisition of the Raman spectra.

Catalytic reactions. Partial oxidation of methanol was carried out at 498 K by using a conventional flowing system with a mixture of CH_3OH, O_2, and N_2 at a ratio of 3/15/82 (mol%). About 10–500 mg of catalyst sample was employed to obtain approximately 20% conversion, except for the MoO_3/Al_2O_3 catalyst system, where higher conversions were used to obtain detectable amounts of partial oxidation products. Prior to the reaction, the catalysts were treated with O_2 at 773 K for 1 h. The reaction products were analyzed by an on-line gas chromatograph which was installed at the outlet of the reactor. The column packings were 1.5 m of Porapak T at 413 K for the separation of CO_2, HCHO, CH_3OCH_3, H_2O, CH_3OH, $HCOOCH_3$, and $(CH_3O)_2CH_2$ and 3 m of Porapak T at 213 K for separation of O_2 and CO. Heat and mass transfer effects were considered using previously determined criteria (46). No heat and mass transfer limitations were indicated from the calculations. The overall activity (mmol g^{-1} h^{-1}) was calculated from the number of moles of methanol converted per hour per gram. The catalytic activity for the different catalysts was converted to turnover frequency, TOF (s^{-1}), which is the moles of methanol converted per mole of Mo atom per second at steady state.

TABLE 1

Surface Properties of Supported Molybdenum Oxide Catalysts

Oxide support	pH[a]	Loading (wt%)	Surface area ($m^2 g^{-1}$)	CO_2 uptake ($\mu mol\ g^{-1}$)
TiO_2(A)	5.99	4.7	61.0 (68.5)[b]	7.5(197.0)[c]
TiO_2(R)	6.01	4.5	45.1 (48.4)	23.0(107.0)
ZrO_2	5.96	5.7	52.9 (54.8)	20.8(336.0)
Al_2O_3	5.98	10.5	162.0(165.0)	27.9(193.0)
SiO_2	5.97	13.0	140.0(160.0)	3.9 (14.8)
MgO	9.30	33.6	166.0 (58.6)	164.0(196.0)

Note. The A and R represent anatase and rutile, respectively.

[a] Final pH of the impregnating solution.

[b] The numbers in parentheses represent the surface areas of the support without MoO_3.

[c] The numbers in parentheses indicate CO_2 uptakes of the oxide supports without MoO_3.

RESULTS

Surface Areas and CO_2 Chemisorption

The surface properties of the supported molybdenum oxide catalysts prepared at pH ~6.0, except for the MoO_3/MgO catalyst, which was prepared at pH 9.3, are presented in Table 1. The numbers in parentheses are surface areas and CO_2 uptakes of the oxide supports without MoO_3. The supported molybdenum oxide catalysts, except the MoO_3/MgO catalyst, possess slightly lower surface areas than the pure oxide supports. It is well established that CO_2 chemisorbs selectively on the OH groups of the oxide support surface (16, 47). A decrease in the amounts of CO_2 chemisorption is observed by addition of molybdenum oxide to the oxide supports with the exception of the MoO_3/MgO catalyst. This result suggests that the surface OH groups of the supports are consumed by interaction with the surface molybdenum oxide species. The MoO_3/MgO catalyst, however, displayed a different trend for the surface area and CO_2 uptake than the other supported molybdenum oxide catalysts: the surface area and CO_2 uptake increase upon the addition of molybdenum oxide to the MgO support. These changes are related to formation of $Mg(OH)_2$ upon contact of MgO with water during impregnation of molybdenum oxide (36) and its subsequent decomposition to high-surface-area MgO upon calcination.

Raman Spectroscopy

MoO_3/Al_2O_3 catalysts. The *in situ* Raman spectra of the MoO_3/Al_2O_3 catalysts under dehydrated conditions, where the adsorbed ambient moisture was desorbed at elevated temperatures, are presented in Fig. 1. The sample prepared at pH 8.50 (4.2 wt%) possesses a strong Raman band at 996 cm^{-1} and two broad Raman bands at 853 and ~299 cm^{-1}. These bands are assigned to the symmetric stretching mode of a terminal Mo=O bond, asymmetric stretching mode of a Mo–O–Mo bond, and bending mode of Mo=O bond for the dehydrated surface molybdenum oxide species on alumina, respectively (8, 25b, 34). The sharp Raman band observed at 996 cm^{-1} for the sample prepared at pH 8.50 (4.2 wt%) shifts to 1003 cm^{-1} as the molybdenum oxide content increases. The sample prepared at pH 5.98 (10.5 wt%) possesses a new weak Raman band at 944 cm^{-1} accompanied by Raman bands at ~865, ~580, and ~210 cm^{-1}. The intensities of these bands increase with further increase in molybdenum oxide content. In addition, these Raman band positions are similar to those of the polymolybdate clusters observed in the Raman spectra under hydrated conditions as well as in an aqueous solution (2, 3, 31). This result suggests that Al_2O_3 may contribute to the stabilization of the polymolybdate clusters at high molybdenum oxide contents. A more detailed investigation is required to understand the effect of the Al_2O_3 support on the stabilization of the polymolybdate clusters upon dehydration.

MoO_3/TiO_2 anatase catalysts. The *in situ* Raman spectra of the MoO_3/TiO_2(A) catalysts under dehydrated conditions are shown in Fig. 2. The strong support Raman features due to the TiO_2(A) phase limit the collection of data below 700 cm^{-1}. The Raman band observed at 799 cm^{-1} is due to the first overtone of the 395 cm^{-1} band of TiO_2(A). The MoO_3/TiO_2(A) catalysts possess a strong

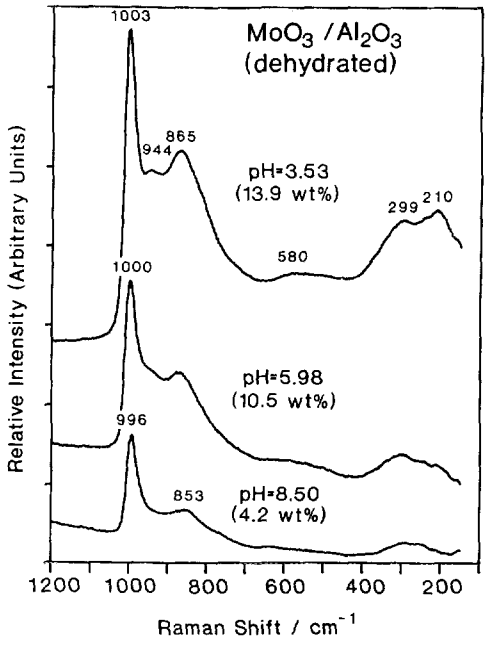

FIG. 1. The *in situ* Raman spectra of the MoO_3/Al_2O_3 catalysts under dehydrated conditions.

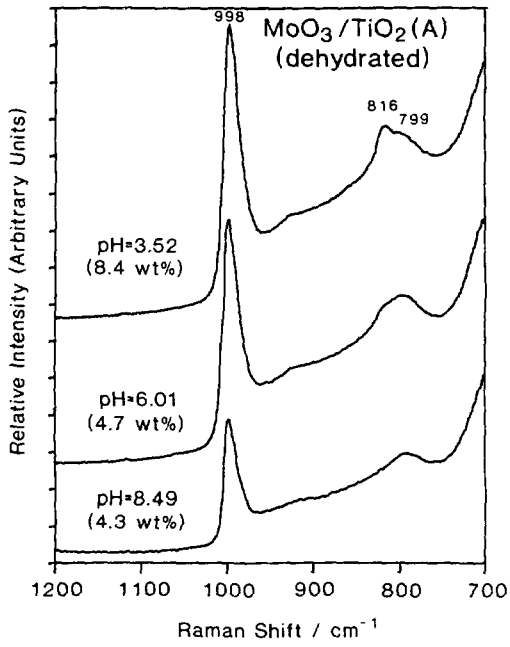

FIG. 2. The *in situ* Raman spectra of the MoO_3/TiO_2 (anatase) catalysts under dehydrated conditions.

Raman band at 998 cm^{-1} independent of molybdenum oxide content which is assigned to the symmetric stretching mode of the terminal Mo=O bond. In addition, the sample prepared at pH 6.01 (4.7 wt%) possesses a very weak Raman band at 816 cm^{-1} due to crystalline MoO_3 and the intensity of this band increases with increasing molybdenum oxide loading (pH 3.52, 8.4 wt% MoO_3).

MoO_3/TiO_2 (rutile) catalysts. The *in situ* Raman spectra of the MoO_3/TiO_2(R) catalysts under dehydrated conditions are presented in Fig. 3. The strong Raman band due to the TiO_2(R) background below 700 cm^{-1} interferes with detection of the Raman bands for the surface molybdate vibrations in this region. The sample prepared at pH 8.52 (3.1 wt%) possesses a Raman band at 994 cm^{-1} for the symmetric stretching mode of the terminal Mo=O bond. At high molybdenum oxide contents, a band due to the symmetric stretching mode of the Mo–O–Mo bond is also present at 867 cm^{-1}. The samples prepared at pH 5.99 (4.5 wt%) and below also exhibit an additional strong Raman band at 984 cm^{-1}. This band is assigned to the symmetric stretching mode of a terminal Mo=O bond which is influenced by coordination of Na (impurity in TiO_2(R), 0.14% (45)) (29, 31, 36) (see Discussion below). Raman bands due to Na_2MoO_4 and crystalline MoO_3 compounds are also observed at 893 and 816 cm^{-1}, respectively, for the sample prepared at pH 3.56 (8.7 wt%). The increase in intensity of the 893 and 984 cm^{-1} Raman bands with decreasing pH of the impregnating solution is due to the increased solubility of Na at lower solution pH values (2a, 29, 31, 36).

MoO_3/ZrO_2 catalysts. The *in situ* Raman spectra of the MoO_3/ZrO_2 catalysts under dehydrated conditions are shown in Fig. 4. The Raman spectra below 700 cm^{-1} were not collected because the strong scattering from the ZrO_2 support dominates this region. The weak Raman band due to the ZrO_2 substrate is observed at 755 cm^{-1}. The MoO_3/ZrO_2 catalysts exhibit Raman bands at 995–1004 and 854–861 cm^{-1} due to the symmetric stretching mode of the terminal Mo=O and asymmetric stretching mode of the Mo–O–Mo bonds, respectively. The Raman bands at 816 and 992 cm^{-1} are associated with crystalline MoO_3 and are observed for the samples prepared at pH below 5.96 (5.7 wt%).

MoO_3/SiO_2 catalysts. The *in situ* Raman spectra of the MoO_3/SiO_2 catalysts under dehydrated conditions are presented in Fig. 5. The MoO_3/SiO_2 catalysts possess strong Raman bands due to crystalline MoO_3 at 992, 816, 664, 335, 281, and 157 cm^{-1} independent of the molybdenum oxide content. This result is attributed to the adsorption of highly polymerized molybdenum oxide clusters as well as microcrystals on SiO_2 during impregnation (31) and their inability to effectively spread upon calcination at 773 K because of a relatively low reactivity and density of the surface OH groups on SiO_2 in comparison to other

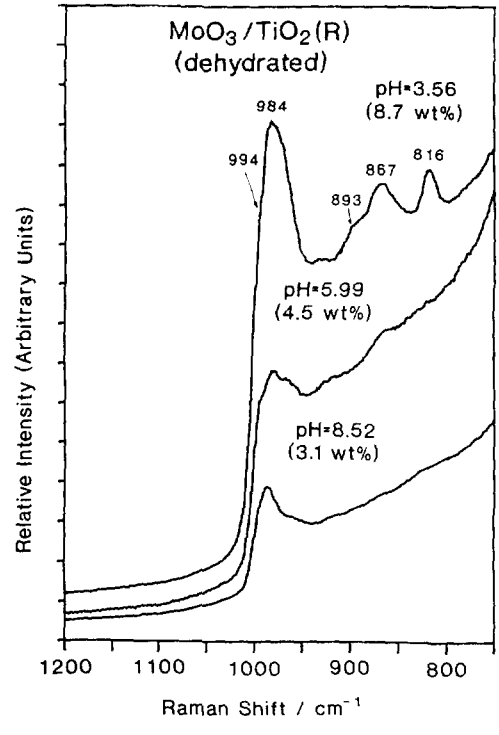

FIG. 3. The *in situ* Raman spectra of the MoO_3/TiO_2 (rutile) catalysts under dehydrated conditions.

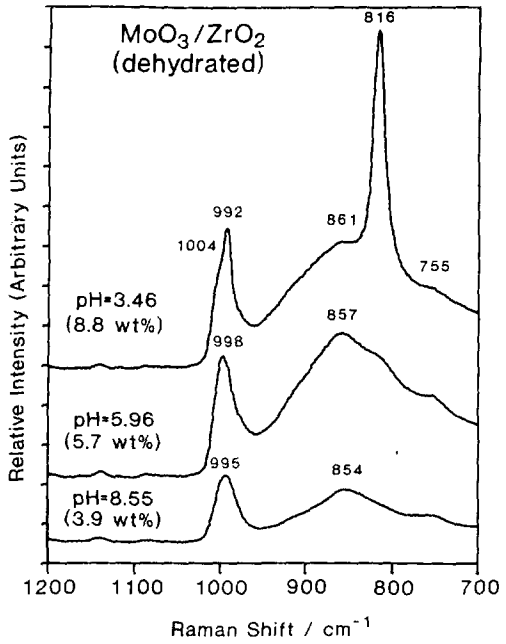

FIG. 4. The *in situ* Raman spectra of the MoO_3/ZrO_2 catalysts under dehydrated conditions.

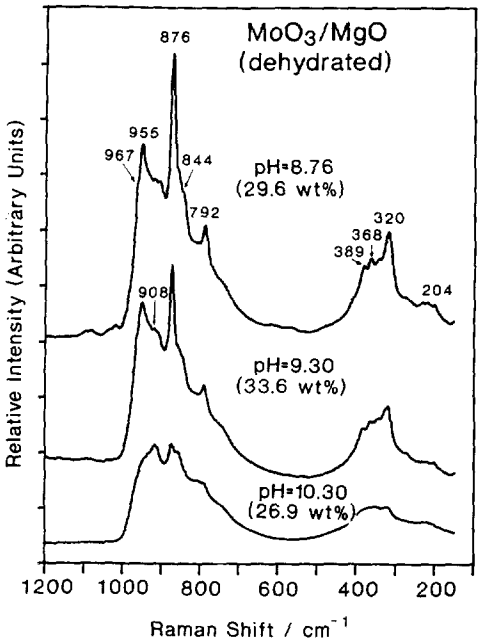

FIG. 6. The *in situ* Raman spectra of the MoO_3/MgO catalysts under dehydrated conditions.

oxide supports (see Table 1). The Raman band due to the surface molybdenum oxide species (ν_s (Mo=O) at 980–990 cm^{-1}) on SiO_2 (8, 17b, 34) may also be present, but would be obscured by the very strong 992-cm^{-1} band of crystalline MoO_3 since the Raman intensity of the crystalline MoO_3 band is significantly greater than that of the surface molybdenum oxide species (16).

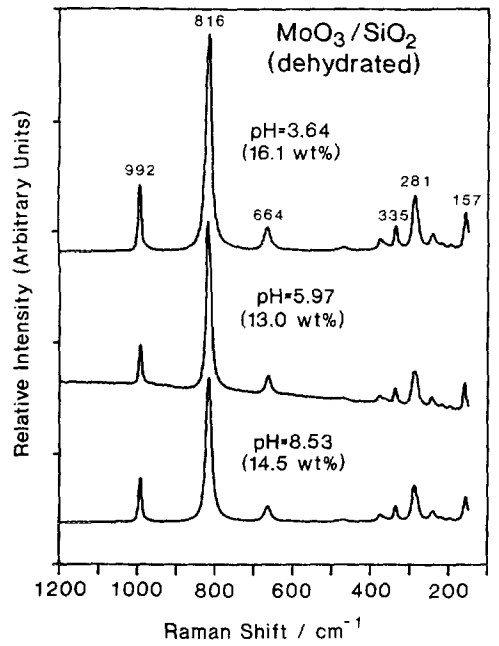

FIG. 5. The *in situ* Raman spectra of the MoO_3/SiO_2 catalysts under dehydrated conditions.

MoO_3/MgO catalysts. The *in situ* Raman spectra of the MoO_3/MgO catalysts under dehydrated conditions are shown in Fig. 6. The catalysts exhibit strong Raman bands at 876, 792, 844, 389, 320, and 204 cm^{-1} corresponding to crystalline $CaMoO_4$ and 967, 955, 908, and 368 cm^{-1} corresponding to crystalline $MgMoO_4$ compounds (19, 29, 31, 36). No Raman band due to the dehydrated surface molybdenum oxide species on MgO is observed (36). Furthermore, the band intensity of the crystalline $CaMoO_4$ and $MgMoO_4$ increases as the pH of the impregnating solution decreases.

Catalytic Reactions

The catalytic activity and selectivity for methanol oxidation over supported molybdenum oxide catalysts at 498 K are shown in Table 2. The catalysts prepared at pH ~6.0, as well as the MoO_3/MgO catalyst prepared at pH 9.30 (33.6 wt%), were used in this investigation. Blank runs were performed on the Pyrex tube packed with quartz wool without any detectable conversions. The overall activities of pure TiO_2(A), TiO_2(R), and ZrO_2 were 1, 2, and 5 mmol g^{-1} h^{-1}, respectively. The pure SiO_2 and MgO supports were essentially inert for methanol oxidation. These reactivity values are minimal in comparison to the reactivity of the supported molybdenum oxide

TABLE 2

Catalytic Activities and Selectivities for Methanol Oxidation on Supported Molybdenum Oxide Catalysts[a]

Oxide support	Loading (wt%)	Total rate (mmol g^{-1} h^{-1})	TOF (10^{-2} s^{-1})	Selectivity[b]			T_{max}[c] (K)
				FA	MF	DME	
TiO_2(A)	4.7	226	22.6	78.1	17.0	4.9	653
TiO_2(R)	4.5	319	28.3	47.5	51.2	1.3	—
ZrO_2	5.7	324	22.7	69.2	26.8	4.0	657
Al_2O_3	10.5	15[d]	0.6[d]	14.0	2.5	83.5[e]	728
SiO_2	13.0	3	0.1	—	—	—	745
MgO	33.6	0	0.0	—	—	—	743

Note. A and R represent anatase and rutile, respectively; FA, MF, and DME represent HCHO, $HCOOCH_3$, and CH_3OCH_3, respectively.

[a] Reaction temperature, 498 K; $CH_3OH/O_2/N_2$ = 3/15/83 (mol%).

[b] Methanol conversion at 20%.

[c] Value of T_{max} were obtained from TPR using 5% H_2/N_2 and heating rates of 5 K min^{-1}. Catalysts possess 1% MoO_3 loading and 100% dispersion with the exception of MgO.

[d] Calculated from the sum of HCHO and $HCOOCH_3$.

[e] The high selectivity of DME for MoO_3/Al_2O_3 is attributed to the support itself.

catalysts under the same reaction conditions (see Table 2). However, the Al_2O_3 support showed a very high activity (90 mmol g^{-1} h^{-1}) for methanol oxidation and 100% selectivity toward dimethyl ether, CH_3OCH_3, because of the presence of surface Lewis acid sites (29). Therefore, the activity of methanol oxidation for the MoO_3/Al_2O_3 catalyst was calculated from the redox products (HCHO and $HCOOCH_3$).

The TOFs for the supported molybdenum oxide catalysts vary with the type of oxide support as presented in Table 2. The TOFs of the MoO_3/SiO_2 and MoO_3/MgO catalysts are not strictly correct since appreciable amounts of crystalline molybdenum oxide phases are present in these samples and molybdenum oxide dispersion was assumed to 100% for these calculations (see Discussion for additional comments). The TiO_2(A and R)- and ZrO_2-supported molybdenum oxide catalysts are the most active catalysts and their TOFs are at least 1–2 orders of magnitude higher than those of the Al_2O_3-, SiO_2-, and MgO-supported molybdenum oxide catalysts. The MoO_3/TiO_2(A) and MoO_3/ZrO_2 catalysts show slightly lower TOFs than MoO_3/TiO_2(R) catalysts due to the presence of some crystalline MoO_3 (TOF of $\sim 2 \times 10^{-2}$ s^{-1}), which is less active than the surface molybdenum oxide species on TiO_2 and ZrO_2 (see the Raman spectra in Figs. 2 and 4) (40). The small amount of Na in the MoO_3/TiO_2(R) catalyst is not expected to significantly affect the catalyst activity since corresponding studies with V_2O_5/TiO_2 catalysts have shown that small amounts of alkali have a minor effect on activity (29). The apparent TOFs of the MoO_3/SiO_2 and MoO_3/MgO catalysts are low due to the lower dispersion of molybdenum oxide on these supports as well as their lower intrinsic TOFs. As mentioned above, bulk crystalline MoO_3 predominates in MoO_3/SiO_2 samples and its TOF is $\sim 2 \times 10^{-2}$ s^{-1}. The TOF for a 1 wt% MoO_3/SiO_2 catalyst, where crystalline MoO_3 is not present and only surface molybdenum oxide species are present, is 3.9×10^{-2} s^{-1}, which is still one order of magnitude lower than that for MoO_3/TiO_2 and MoO_3/ZrO_2 (see Table 2). The MoO_3/MgO catalysts do not show any catalytic activity due to the presence of crystalline $MgMoO_4$ and $CaMoO_4$ compounds which apparently are totally unreactive (see Fig. 6). As shown in Table 2, the TOF for methanol oxidation correlates with the reducibility of the supported molybdenum oxide catalysts (represented as T_{max}): the more reducible molybdenum oxide catalysts possess higher TOFs while the less reducible molybdenum oxide catalysts exhibit lower TOFs.

The main reaction product during methanol oxidation is formaldehyde (HCHO) and the selectivity of methyl formate ($HCOOCH_3$) is next in abundance for the MoO_3/TiO_2(A) and MoO_3/ZrO_2 catalysts. The MoO_3/TiO_2(R) catalyst possesses a higher selectivity toward $HCOOCH_3$ than the MoO_3/TiO_2(A) catalysts. The different $HCOOCH_3$ selectivities for MoO_3/TiO_2(A) and MoO_3/TiO_2(R) suggest that the presence of alkali also affects the formation of $HCOOCH_3$. Only small amounts of dimethyl ether (CH_3OCH_3), produced by surface acid sites, are observed for these catalysts (29). However, the MoO_3/Al_2O_3 catalyst possesses a very high selectivity for CH_3OCH_3 (83.5% selectivity) due to the surface acidic properties of this catalyst.

DISCUSSION

Recently, Kim *et al.* (31) demonstrated that the surface molybdenum oxide species under ambient conditions are

hydrated and essentially in an aqueous medium. Consequently, the structure of the hydrated surface molybdenum oxide overlayer follows the molybdenum oxide aqueous chemistry as a function of the net surface pH at point of zero charge (PZC) (18, 31, 32). The net surface pH at PZC under ambient conditions is determined by the specific oxide support, surface metal oxide content, and type and amounts of impurities on the oxide support (18). Upon dehydration, the adsorbed water molecules desorb at elevated temperature and the surface molybdenum oxide species on the oxide supports become dehydrated. Therefore, the net surface pH at PZC does not dominate under dehydrated conditions because this mechanism is applicable only when water is present.

The first *in situ* Raman spectroscopic studies on supported molybdenum oxide catalysts under dehydrated conditions were reported by Wang *et al.* (2a). Subsequently, Stencel *et al.* (21) and Wachs *et al.* (2d, 8, 17, 19, 20, 30, 34) published a large number of papers on this topic. Wang *et al.* (2a, 2d) and Stencel *et al.* (21) suggested that the Raman band shift of the terminal Mo=O bond toward the high wavenumber region upon dehydration is due to the additional distortion imposed on the surface molybdenum oxide species when the adsorbed moisture is removed and reflects a shortening of the terminal Mo=O bond of the surface molybdenum oxide species. Wachs *et al.* (8, 17, 19, 20, 30, 34), however, have proposed that quite different molybdenum oxide species are formed on the oxide supports under dehydrated conditions.

Recently, Roark *et al.* (34) and de Boer *et al.* (8) have provided direct evidence that different molybdenum oxide species are formed on the silica surface upon dehydration. The hydrated surface molybdenum oxide species on silica possesses Raman bands at 948 (ν_s (Mo=O)) and 881 cm^{-1} (ν_{as} (Mo–O–Mo) due to the polymolybdate clusters, mainly $Mo_7O_{24}^{6-}$, and these bands disappear upon dehydration with a new Raman band observed at 986 cm^{-1} (ν_s (Mo=O)). The absence of the Mo–O–Mo bond (881 cm^{-1}) for the dehydrated MoO_3/SiO_2 catalysts indicates that different molybdenum oxide species are present under dehydrated conditions. de Boer *et al.* (8) also confirmed the disappearance of the Mo–O–Mo bond upon dehydration from an *in situ* EXAFS study for the MoO_3/SiO_2 system. Roark *et al.* (49) showed with *in situ* IR spectroscopy that the introduction of water to the dehydrated MoO_3/SiO_2 catalysts results in the hydrolysis of the bridging oxygen Mo–O–Si bond which regenerates the SiO_2 surface hydroxyls. Upon dehydration, these surface SiO_2 hydroxyls are consumed by interaction with the surface molybdenum oxide species. In addition, Payen *et al.* (25c) have reported that the sulfiding process over MoO_3/Al_2O_3 catalysts proceeds via different intermediates in the presence and absence of adsorbed water on the catalyst. The above results strongly support the conclusion that different molybdenum oxide species are formed on the oxide support under hydrated/dehydrated conditions: water molecules strongly influence the molecular structure of the surface molybdenum oxide species on oxide supports.

A number of studies on the assignment of Raman band positions under dehydrated conditions have been reported (2a, 2d, 8, 17–21, 30, 34). However, there are still disagreements regarding the interpretation of the Raman bands: whether the surface molybdenum oxide species possesses monooxo (octahedral) or dioxo (tetrahedral) molybdenum oxide structures. Oyama *et al.* (35) proposed that the surface molybdenum oxide species on the silica surface possesses dioxo molybdenum oxide structures. Wachs *et al.* (8, 17, 19, 20, 30, 34), however, proposed that monooxo molybdenum oxide species are present independent of the type of oxide support. Recently, Vuurman *et al.* (30) reported that the 10 wt% MoO_3/Al_2O_3 catalyst under dehydrated conditions possesses only one Raman and one IR band at ~1000 cm^{-1} (ν_s (Mo=O)). Similarly, de Boer (8) also showed that the MoO_3/SiO_2 catalyst under dehydrated conditions possesses identical Raman and IR bands for the terminal Mo=O bond at 986 cm^{-1} by performing corresponding *in situ* Raman and IR spectroscopic studies. This observation is significant since according to Raman/IR vibrational selection rules this coincidence should occur only for monooxo species (50). A dioxo (O=Mo=O) molybdenum oxide species should give rise to two Raman and IR bands for the symmetric and asymmetric stretching modes since IR is more sensitive to the asymmetric mode than the symmetric mode of the O=Mo=O bond and Raman should show an opposite trend (50). Moreover, Cornac *et al.* (51) confirmed that the surface molybdenum oxide species on silica possess monooxo molybdenum oxide species by conducting an $^{18}O_2$–$^{16}O_2$ isotopic study. The coordination of the surface molybdenum oxide species on the oxide supports is not immediately apparent just from Raman spectroscopic studies. At present, however, it is assumed that the surface molybdenum oxide species possess an octahedral coordination because an octahedrally coordinated monooxo molybdate species is quite common and no monooxo molybdate species with tetrahedral coordination is known (19). In addition, de Boer *et al.* (8) showed that the MoO_3/SiO_2 catalysts under dehydrated conditions possess monooxo molybdate species with octahedral coordination by *in situ* Raman and XANES studies.

The dehydrated MoO_3/support (Al_2O_3, TiO_2, and ZrO_2) catalysts possess an additional Raman band at 853–865 cm^{-1} (see Figs. 1–4) and the relative intensity of this band increases with increasing surface molybdenum oxide coverage. As stated previously, the Raman band at 853–865 cm^{-1} for the MoO_3/support system is attributed to the asymmetric stretching mode of the Mo–O–Mo bond for the surface molybdenum oxide species on oxide supports. The broadening of this band suggests that the

MoO_3/support catalysts possess surface molybdenum oxide species with a distribution of Mo–O–Mo bond distances. The absence of a strong Raman band due to the Mo–O–Mo bond for MoO_3/TiO_2(A) catalysts at 853–865 cm^{-1} indicates that the surface molybdenum oxide species on TiO_2(A) are less polymerized than the MoO_3/support (Al_2O_3, TiO_2(R), and ZrO_2) catalysts.

The MoO_3/TiO_2(R) samples prepared at a pH below 5.99 (4.5 wt%) possess a new Raman band at 984 cm^{-1} which indicates the formation of a new surface molybdenum oxide species on TiO_2(R). Wachs *et al.* (29, 30) have reported that the acidic additives (MoO_3, WO_3, and Nb_2O_5) do not significantly influence the structure of the surface vanadium oxide species on oxide support under dehydrated conditions. Furthermore, Deo and Wachs (29) observed that addition of basic additives (K_2O) to V_2O_5/TiO_2 catalysts results in a decrease in the Raman band of the V=O bond to lower wavenumbers due to the direct coordination of potassium to the terminal V=O bond. The band at 984 cm^{-1} for MoO_3/TiO_2(R), similarly, is attributed to the symmetric stretching mode of a terminal Mo=O bond whose bond length is increased by direct coordination with Na since the TiO_2(R) contains 0.14% Na_2O as impurity (17, 29, 48).

The MoO_3/MgO catalysts possess strong Raman features due to crystalline $CaMoO_4$ and $MgMoO_4$ and the intensity of these bands increases with decreasing pH of the impregnating solution. No surface molybdenum oxide species is observed for the MoO_3/MgO catalysts. It is well known that the solubility of CaO and MgO increases with decreasing pH and, consequently, can make compounds with molybdenum oxide species present in the aqueous solution at low pH (2a, 17, 19, 29, 31, 36). This suggests that the high solubility of MgO and CaO impurities as well as the strong acid–base interaction between molybdenum oxide and MgO and CaO is responsible for the formation of crystalline $MgMoO_4$ and $CaMoO_4$. Essentially identical observations were made for other acidic oxides (V_2O_5, CrO_3, WO_3, and Re_2O_7) supported on MgO (2a, 29, 52). The observation of the Raman band due to crystalline Na_2MoO_4 (893 cm^{-1}) for the MoO_3/TiO_2(R) catalyst, discussed above, also coincides with low pH conditions and directly confirms the interaction of Na and Mo on the TiO_2(R) samples.

Wang and Hall (2) have proposed that the pH of the impregnating solution is not only a very essential parameter for regulating the adsorbed amounts of metal oxide species, but also an important factor for controlling the adsorption species on the alumina surface. They have also suggested that molybdenum oxide species at a given pH of the impregnating solution are adsorbed intact on the alumina surface (2). However, the *in situ* Raman and EXAFS studies showed that totally different surface molybdenum oxide species are formed on the oxide support under hydrated/dehydrated conditions (8, 15, 30, 34). Under hydrated conditions, the polymolybdate clusters such as $Mo_7O_{24}^{6-}$ and/or $Mo_8O_{26}^{4-}$ are present on the oxide support (18, 29–31) as a function of the net surface pH at PZC. Upon dehydration, the polymolybdate clusters are unstable and decompose to form dehydrated surface molybdenum oxide species with one terminal Mo=O bond and several bridging Mo–O–support bands. The similarity of the molybdenum–oxygen vibrations of the surface molybdenum oxide species on the different oxide supports suggests that essentially the same surface molybdenum oxide species is present with the exception of the SiO_2 and MgO supports, where crystalline molybdate phases predominate. Furthermore, the dehydration/rehydration process is reversible (30).

The methanol oxidation reaction studies demonstrated that the TOF for supported molybdenum oxide catalysts is strongly dependent on the specific oxide support and decreases in the following order: TiO_2(R) $\simeq$ TiO_2(A) $\simeq$ $ZrO_2 \gg Al_2O_3 > SiO_2 >$ MgO. The lower apparent TOFs of MoO_3/SiO_2 and MoO_3/MgO are also partially due to the fact that these catalysts do not possess 100% dispersion of molybdenum oxide. As already mentioned above, the MoO_3/Al_2O_3 catalyst possesses essentially the same surface molybdenum oxide structure as MoO_3/TiO_2(A and R) and MoO_3/ZrO_2 catalysts, but the reactivity is more than one order of magnitude lower for MoO_3/Al_2O_3 (see Table 2). Furthermore, the TOF correlates with the reducibility of the supported molybdenum oxide catalysts; the more reducible catalysts (MoO_3/TiO_2(A and R) and MoO_3/ZrO_2) possess a higher TOF than the less reducible catalysts (MoO_3/Al_2O_3) (see Table 2). A similar observation has been made for other supported surface metal oxide phases (V_2O_5, CrO_3, and Re_2O_7) (33), which confirms that this phenomenon is related to the specific oxide support and not to the specific surface metal oxide overlayer.

Recent *in situ* Raman spectroscopic studies by Hu and Wachs (53) indicate that the extent of reduction of the surface molybdenum oxide species during methanol oxidation reaction is strongly dependent on the type of oxide support. The surface molybdenum oxide species on the ZrO_2 and Al_2O_3 supports undergo a substantial reduction (decrease of the Raman signal associated with the Mo=O bond) during methanol oxidation (CH_3OH/O_2/He at 300°C), whereas, only a minor degree of reduction is observed for TiO_2 for the surface molybdenum oxide species. These observations suggest that the type of oxide support controls the extent of reduction of the surface molybdenum oxide species during methanol oxidation. However, the extent of reduction of the surface molybdenum oxide species during methanol oxidation ($Al_2O_3 \simeq ZrO_2 > TiO_2$) does not correlate with the reducibility of the supported molybdenum oxide catalyst ($ZrO_2 \simeq TiO_2 > Al_2O_3$) as determined by temperature programmed reduction. In addition, these *in situ* reaction studies also

reveal that not all surface molybdenum oxide sites are participating simultaneously in the methanol oxidation reaction.

The catalysts which are dominated by crystalline molybdate phases (MoO_3/SiO_2 and MgO_3/MgO) are significantly less active than the catalysts which predominantly possess surface molybdenum oxide species (MoO_3TiO_2(A and R), MoO_3/ZrO_2, and MoO_3/Al_2O_3) as shown in Table 2. The low apparent TOF for MoO_3/SiO_2 is due to the lower reactivity and dispersion of MoO_3 crystallites since only trace amounts of surface molybdenum oxide species may be present (~5%). The low apparent TOF for MoO_3/MgO is primarily due to the essentially unreactive $MgMoO_4$ and $CaMoO_4$ phases since surface molybdenum oxide species are not usually present on MgO because of the reactivity of this support (53). Thus, increasing the dispersion of the $MgMoO_4$ and $CaMoO_4$ crystalline phases will not increase the reactivity of these essentially inert phases.

The origin of the support effect on the reactivity of the methanol oxidation reaction, however, is not fully understood in the literature. With the structural information derived from *in situ* Raman spectroscopic studies, the difference in the reactivity is not a structural factor since the surface structure of the molybdenum oxide species is essentially independent of the specific oxide support. In addition, the activation energy for methanol oxidation is almost the same (18–22 Kcal mol^{-1}) for all the supported metal oxide (MoO_3, V_2O_5, CrO_3, and Re_2O_7) catalysts (33). This activation energy corresponds to that expected for breaking of the C–H bond of the surface methoxide, adsorbed CH_3O and is independent of the specific oxide support (54, 55). A number of previous studies suggested that the terminal Mo = O bond is influenced by the specific oxide support which is involved in the methanol oxidation reaction (41, 54). The Raman band position is directly related to bond strength and shorter bonds correspond to higher Raman band positions (see Figs. 1–4 and Table 2). The present investigation, however, reveals that there is no relationship between the reactivity of the catalysts and the Raman band positions of terminal M = O (990–1000 cm^{-1}) bonds. Therefore, the origin of the support effect on the reactivity of the MoO_3/support catalysts is most probably related to the Mo–O–support bond since this bond is directly influenced by the oxide support. Similar observations and conclusions were recently made for other supported metal oxide catalyst systems (33).

The observation of different TOFs (1–2 orders of magnitude) for the MoO_3/support catalysts with respect to the specific oxide support and the similar activation energies suggests that the number of active sites and/or the activity per site during methanol oxidation are responsible for the origin of the support effect (29). The number of active sites, taken as surface molybdenum oxide sites being reduced during methanol oxidation, is strongly dependent on the nature of the oxide support as revealed by *in situ* Raman studies during methanol oxidation. The MoO_3/ZrO_2 and MoO_3/Al_2O_3 catalysts which show similar extent of reduction of the surface molybdenum oxide species during the *in situ* methanol oxidation Raman studies possess catalytic activities that differ by over one order of magnitude (see Table 2). Hence, the activity per site appears to be responsible for the different TOFs of these two supported molybdenum oxide catalysts ($MoO_3/ZrO_2 \gg MoO_3/Al_2O_3$). The MoO_3/TiO_2 catalyst does not, however, show the same extent of reduction of the surface molybdenum oxide species as the MoO_3/ZrO_2 but both catalysts possess very similar TOFs. Thus, both the activity per site and number of active sites are playing an important role in determining the relative TOF of the surface molybdenum oxide species supported on TiO_2 and ZrO_2. Furthermore, it appears that from the high TOF of the MoO_3/TiO_2 catalyst and the low extent of reduction of the surface molybdenum oxide species on TiO_2 during methanol oxidation that the activity per site for the MoO_3/TiO_2 catalyst must be greater than that for MoO_3/ZrO_2. Thus, the activity per site appears to be more significant in determining the overall TOF of supported molybdenum oxide species.

CONCLUSIONS

The surface molybdenum oxide species on different oxide supports (Al_2O_3, TiO_2, and ZrO_2) possess a highly distorted molybdenum oxide species with one short Mo=O bond (monooxo species) independent of the molybdenum oxide content. The MoO_3/SiO_2 catalysts primarily contain crystalline MoO_3 because of the lower density and reactivity of the silica surface OH groups. The MoO_3/MgO catalysts possess crystalline $MgMoO_4$ and $CaMoO_4$ because of the high solubility of MgO/CaO impurity and the strong interaction between molybdenum oxide and MgO/CaO in aqueous solutions. The methanol oxidation reaction studies showed that the catalytic activity is strongly dependent on the specific oxide support.

The current findings from *in situ* Raman spectroscopy suggest that the oxide support controls the reactivity of the surface molybdenum oxide species during redox reactions by controlling the number of active sites and activity per site which are specific to a particular oxide support. The influence of the oxide support on the activity per site appears to be the dominant factor controlling the catalytic reactivity. The oxide support also affects the reactivity by influencing the dispersion of the supported molybdenum oxide phase (as in the case MoO_3/SiO_2, where crystalline MoO_3 is almost exclusively formed) and the formation of unreactive molybdenum compounds (as in the case of MoO_3/SiO_2, where $MgMoO_4$ and $CaMoO_4$ are formed).

ACKNOWLEDGMENT

Du Soung Kim acknowledges Professor Jae Sung Lee and Dr. Sang Young Lee at POSTECH in Korea for the TPR measurement.

REFERENCES

1. Thomas, C. L., *in* "Catalytic Processes and Proven Catalysts." Academic Press, New York, 1970.
2. (a) Wang, L., Ph.D. thesis, University of Wisconsin, 1982; (b) Wang, L., and Hall, W. K., *J. Catal.* **77,** 232 (1982); (c) Wang, L., and Hall, W. K., *J. Catal.* **66,** 251 (1980); (d) Chan, S. S., Wachs, I. E., Murrell, L. L., Wang, L., and Hall, W. K., *J. Phys. Chem.* **88,** 5831 (1984).
3. Ng, K. Y. S., and Gulari, E., *J. Catal.* **92,** 340 (1985).
4. (a) Jeziorowski, H., and Knozinger, H., *J. Phys. Chem.* **83,** 1166 (1979); (b) Knozinger, H., and Jeziorowski, H., *J. Phys. Chem.* **82,** 2002 (1978).
5. Liu, Y. C., Griffin, G. L., Chan, S. S., and Wachs, I. E., *J. Catal.* **94,** 108 (1985).
6. Kakuta, N., Tohji, K., and Udagawa, Y., *J. Phys. Chem.* **92,** 2583 (1988).
7. Iwasawa, Y., Sato, Y., and Kuroda, H., *J. Catal.* **82,** 289 (1983).
8. (a) de Boer, M., van Dillen, A. J., Koningsberger, D. C., Geus, J. W., Vuurman, M. A., and Wachs, I. E., *Catal. Lett.* **11,** 227 (1991); (b) De Boer, M., Ph.D. thesis, The University of Utrecht, 1992.
9. Chieu, N. S., Bauer, S. H., and Johnson, M. F., *J. Catal.* **89,** 226 (1984); **98,** 32 (1986).
10. Clausen, B. S., Topsøe, H., Candia, R., Christiansen, F., *J. Phys. Chem.* **85,** 3868 (1981).
11. (a) van Veen, J. A. R., Hendriks, P. A. J. M., Romers, E. J. G. M., and Andrea, R. R., *J. Phys. Chem.* **94,** 5275 (1990); (b) Van Veen, J. A. R., de Wit, H., Emeis, C. A., and Hendriks, P. A. J. M., *J. Catal.* **107,** 579 (1987).
12. Shirley, W. M. Z., *Phys. Chem. (Munich)* **152,** 41 (1987).
13. (a) Edwards, J. C., and Ellis, P. D., *Langmuir* **7,** 2117 (1991); (b) Edwards, J. C., Adams, R. D., and Ellis, P. D., *J. Am. Chem. Soc.* **112,** 8349 (1990).
14. Luthra, N. P., and Chang, W. C., *J. Catal.* **107,** 154 (1984).
15. Haller, G., unpublished results.
16. Kim, D. S., Kurusu, Y., Wachs, I. E., Hardcastle, F. D., and Segawa, K., *J. Catal.* **120,** 325 (1989).
17. (a) Williams, C. C., Ekerdt, J. G., Jehng, J. M., Hardcastle, F. D., Turek, A. M., and Wachs, I. E., *J. Phys. Chem.* **95,** 8781 (1991); (b) Williams, C. C., Ekerdt, J. G., Jehng, J. M., Hardcastle, F. D., and Wachs, I. E., *J. Phys. Chem.* **95,** 8791 (1991).
18. Deo, G., Wachs, I. E., *J. Phys. Chem.* **95,** 5889 (1991).
19. Hardcastle, F. D., and Wachs, I. E., *J. Raman Spectrosc.* **21,** 683 (1990).
20. Machej, T., Haber, J., Turek, A., and Wachs, I. E., *Appl. Catal.* **70,** 115 (1991).
21. (a) Stencel, J. M., Makovsky, L. E., Sarkus, T. A., de Varies, J., Thomas, R., and Moulijn, J. A., *J. Catal.* **90,** 314 (1984); (b) Stencil, J. M., *in* "Raman Spectroscopy for Catalysis." Van Nostrand–Reinhold, New York, 1989.
22. Brown, F. R., Makovsky, L. E., and Rhee, K. H., *J. Catal.* **50,** 162 (1977).
23. Quincy, R. B., Houalla, M., and Hercules, D. M., *J. Catal.* **106,** 85 (1987).
24. Cheng, C. P., and Schrader, G. L., *J. Catal.* **60,** 274 (1979).
25. (a) Kasztelan, S., Payen, E., Thoulhoat, H., Grimblot, J., and Bonnelle, J. P., *Polyhedron* **5,** 157 (1986); (b) Payen, E., Kasztelan, S., Grimblot, J., and Bonnelle, J. P., *J. Raman Spectrosc.* **17,** 233 (1986); (c) Payen, E., Kasztelan, S., Houssenbay, S., Azymanski, R., and Grimblot, J. P., *J. Phys. Chem.* **93,** 6501 (1989).
26. Sombert, B., Dhamelincourt, P., Wallert, F., Muller, A. C., Bouquet, M., and Grosmangin, J., *J. Raman Spectrosc.* **9,** 291 (1980).
27. Madema, J., van Stam, C., de Beer, V. J. J., Konings, A. J. A., and Koningsberger, D. C., *J. Catal.* **53,** 386 (1978).
28. Iannibello, A., Marengo, S., Trifiro, F., and Villa, P. L., *in* "Preparation of Catalysts. II. Scientific Basis for the Preparation of Heterogeneous Catalysts" (B. Delmon, P. Grange, P. Jacobs, and G. Poncelet, Eds.), p. 65. Elsevier, Amsterdam, 1979.
29. (a) Deo, G., Ph.D. thesis, Lehigh University, 1993; (b) Deo, G., and Wachs, I. E., J. Catal., *J. Catal.* **146,** 323 (1994); (c) Deo, G., and Wachs, I. E., *J. Catal.* **146,** 335 (1994).
30. (a) Vuurman, M. A., Ph.D. thesis, University of Amsterdam, 1992; (b) Vuurman, M. A., and Wachs, I. E., J. Phys. Chem., **96,** 5008 (1992).
31. Kim, D. S., Segawa, K., Soeya, T., and Wachs, I. E., *J. Catal.* **136,** 539 (1992).
32. Kohler, S. D., Ekerdt, J. G., and Kim, D. S., and Wachs, I. E., *Catal. Lett.* **16,** 231 (1992).
33. (a) Wachs, I. E., Deo, G., Kim, D. S., Vuurman, M. A., and Hu, H., *in* "Proceedings 10th International Congress on Catalysis, Budapest, 1992," Vol. A, p. 543. Elsevier, Amsterdam, 1993; (b) Deo, G., and Wachs, I. E., *J. Catal.* **129,** 307 (1991); (c) Wachs, I. E., Deo, G., Vuurman, M. A., Hu, H., Kim, D. S., and Jehng, J. M., submitted for publication.
34. Roark, R. D., Kohler, S. D., Ekerdt, J. G., Kim, D. S., and Wachs, I. E., *Catal. Lett.* **16,** 77 (1992).
35. (a) Desikan, A. N., Huang, L., and Oyama, S. T., *J. Phys. Chem.* **95,** 10050 (1991); (b) Desikan, A. N., and Oyama, S. T., *Chem. Soc. Chem. Commun.* **88,** 3357 (1992).
36. Chang, S. C., Leugers, M. A., and Bare, S. R., *J. Phys. Chem.* **96,** 10358 (1992).
37. Volta, J. C., Portefaix, J. L., *Appl. Catal.* **18,** 1 (1985).
38. (a) Tatibouet, J. M., Germain, J. M., *J. Catal.* **82,** 240 (1983); (b) Tatibouet, J. M., and Germain, J. M., *J. Catal.* **72,** 375 (1981).
39. Ohuchi, F., Firment, L. E., Chowdhry, U., and Ferretti, A., *J. Vac. Sci. Technol. A* **2,** 1022 (1984).
40. (a) Segawa, K., Soeya, T., and Kim, D. S., *Sekiyu Gakkashi* **33,** 347 (1990); (b) Kim, D. S., Ph.D. thesis, Sophia University, Tokyo, 1990.
41. Louis, C., Tatibouet, J. M., and Che, M., *J. Catal.* **109,** 354 (1988).
42. Roozeboom, F., Cordingley, P. D., and Gellings, P. J., *J. Catal.* **68,** 464 (1981).
43. Bond, G. C., Zurita, P. J., Flamerz, S., Gellings, P. Z., Bosch, H., van Ommen, J. G., and Kip, B. J., *Appl. Catal.* **22,** 361 (1986).
44. Murakami, Y., *in* "Preparation of Catalysts, III" (G. Ponceit, P. Grange, and P. A. Jacobs, Eds.), Studies in Surface Science and Catalysis Series, p. 775. Elsevier, Amsterdam, 1983.
45. Nakao, Y., Iizuka, T., Hattori, H., and Tanabe, K., *J. Catal.* **57,** 1 (1979).
46. Froment, G. F., and Bischoff, K. B., *in* "Chemical Reactor Analysis and Design," Chap. 3, p. 141. Wiley, New York, 1979.
47. Segawa, K., and Hall, W. K., *J. Catal.* **77,** 221 (1982).
48. Japan Reference Catalysts Committee, *in* "Proceedings 12th Japan Reference Catalysts Conference on Surface Property and Catalysis of Japan Reference Titanium Oxide, Nagasaki, 1989," p. 2.
49. Roark, S. D., Kohler, S. D., Ekerdt, J. G., *Catal. Lett.* **16,** 71 (1992).
50. Nakamoto, K., *in* "Infrared and Raman Spectra of Inorganic and Coordination Compounds," 4th Ed. Wiley, New York, 1992.
51. Cornac, M., Janin, A., and Lavalley, J. C., *Polyhedron* **5,** 183 (1983).
52. (a) Kim, D. S., and Wachs, I. E., unpublished results; (b) *J. Catal.* **141,** 419 (1993); (c) *J. Catal.* **142,** 166 (1993).
53. Wachs, I. E., and Hu, H., unpublished results.
54. Yang, T. J., and Lunsford, J. H., *J. Catal.* **103,** 55 (1987).
55. Fareneth, W. E., Ohuchi, F., Staley, R. H., Chowdhry, U., and Sleight, A. W., *J. Phys. Chem.* **89,** 2493 (1985).